

Electronic Interactions in Photosynthetic Light-Harvesting Complexes: The Role of Carotenoids

Gregory D. Scholes*,†

Department of Chemistry, Imperial College of Science, Technology and Medicine, Exhibition Road, London SW7 2AY, United Kingdom

Richard D. Harcourt‡

School of Chemistry, The University of Melbourne, Parkville, Victoria 3052, Australia

Graham R. Fleming*,§

Department of Chemistry and The James Franck Institute, The University of Chicago, 5735 S. Ellis Ave., Chicago, Illinois 60637

Received: December 3, 1996; In Final Form: March 26, 1997[®]

The origin and distance dependence of the electronic interactions which promote energy transfer within photosynthetic light-harvesting complexes is investigated. A model based on localized molecular orbitals is related to canonical molecular orbital calculations, therefore demonstrating its practical utility and allowing us to interpret the results of CAS-SCF calculations of the coupling between donor–acceptor pairs. We then focus on the mechanism of energy transfer involving the carotenoid 2^1A_g (S_1) electronic state: [carotenoid (2^1A_g) (Car) to carotenoid (2^1A_g)] and [carotenoid (2^1A_g) to bacteriochlorophyll (Q_y) (Bchl)] interactions. The Car–Car coupling is found to involve reasonably long-range interaction terms, with a primary contribution from dispersion-type interactions, which have an R^6 distance dependence. The primary contributor to the Car–Bchl $S_1 \rightarrow S_1$ energy transfer mechanism is suggested to be proportional to the product of dipole–dipole and polarization interactions. In neither case does the electronic interaction resemble the Dexter exchange integral in origin or distance dependence. Some model CAS-SCF calculations of electronic interactions in 2,4,6-octatriene dimers are presented which support the predictions of the theory: the calculated interaction is found to be (i) small in comparison to the overlap-dependent triplet–triplet interaction at close separations; (ii) small in comparison to a dipole–dipole (S_2) interaction at all separations; and (iii) quite weakly distance dependent at larger separations. The implications for the role of carotenoids in photosynthetic light-harvesting complexes are discussed.

1. Introduction

Electronic energy transfer^{1–4} (EET) provides a means for the efficient transport of absorbed light energy from an array of light-harvesting pigments to a reaction center, or trap site.^{5–8} Such a system is ubiquitous in nature, providing a key contribution to the highly efficacious solar energy conversion system in green plants and photosynthetic bacteria. Recent observations of the time scales of energy transfer processes in these natural light-harvesting complexes have raised questions regarding the mechanisms promoting energy migration.⁸ Surprisingly, it is only recently that we have begun to understand properly the mechanisms which promote EET even in model bichromophores.^{9–15}

The high-resolution structure¹⁶ of the bacterial peripheral light-harvesting protein LH2 (together with the lower resolution structure¹⁷ of LH1) suggests that strong interactions are likely to couple the symmetrically-arranged chromophores within the structure. This is supported by the ultrafast “rates” of energy transfer measured or suggested by experiment.^{18–20} In the B850 ring of LH2 it is clear that bacteriochlorophyll *a* (Bchl *a*) chromophores approach to approximately 3.4–4.0 Å. In fact,

the X-ray structure data indicate that electron density is shared within alternating Bchl *a* pairs. The corollary is that interactions which are mediated by interchromophore orbital overlap should be considered when modeling EET and exciton interactions. It is therefore probable that the form of the electronic interaction which couples these chromophores in an excited state should deviate significantly from that estimated by the dipole–dipole model.^{11,13,15} Even if this is not so, for example, for B800, then use of the dipole–dipole model should be carefully justified. Consideration of the origin and magnitude of the electronic coupling between the constituent chromophores of B850 is relevant to the recent debate over “delocalisation length” in B850.^{18,21,22} Such issues are, of course, also pertinent to the analysis of strongly-coupled multichromophoric systems such as FMO complexes²³ and PSII.²⁴

We describe in section 3 a methodology for determining the electronic factors which is based on a detailed elucidation of their form (which was established recently²²) but employs a molecular orbital-based calculation of dimer excited states. (Previously we used a specialised multiconfiguration valence bond program.¹³) The advantage is that calculations on very large systems are possible, using accessible quantum chemical programs. We use this approach to interpret the results of CAS-SCF calculations of the interactions within a model polyene dimer. Of course, experiment may ultimately reveal the microscopic details of LH2 functionality, but at this stage

* Corresponding authors. Present address: Department of Chemistry, University of California, Berkeley, CA 94720-1460.

† E-mail: g.scholes@ic.ac.uk.

‡ E-mail: harcus@rubens.its.unimelb.edu.au.

§ E-mail: Fleming@cchem.berkeley.edu.

® Abstract published in *Advance ACS Abstracts*, August 15, 1997.

reliable quantum mechanical calculations can illuminate some key issues, feeding back into experimental analysis.

An important constituent of LH2, indeed most photosynthetic systems, are the carotenoids.^{25,26} The *all-trans* rhodopin glucoside carotenoid present in LH2 spans the entire width of the membrane and appears to be in van der Waals contact with Bchl *a* pigments of the B800 and B850 rings. The implications for energy transfer, carotenoid to Bchl *a*, or B800 to B850 via a superexchange mechanism, have yet to be elucidated. Some recent experimental studies of the role of carotenoids in the light-harvesting apparatus have focused on *Rh. Sphaeroides*.^{27,28} A complementary theoretical study of the electronic coupling between neurosporene and Bchl *a* has also been presented.²⁹ In section 4 we investigate in detail the origin of interactions involving the carotenoid (or polyene) 2^1A_g state; we report the results of some model calculations of the coupling in octatriene dimers and some initial calculations of rhodopin glucoside in section 5, and then discuss the implications for LH2 in section 6.

In the present work we address the following issues: (i) How are electronic couplings manifest between chlorophylls in light harvesting complexes; in particular, what is the role of charge transfer configurations (especially with respect to spectral shifts, splittings, superradiance, etc.)? (ii) How can we estimate them using quantum chemical methods? (iii) What is the mechanism for energy transfer from the carotenoid 2^1A_g state to another carotenoid or to a chlorophyll? (iv) What role do the carotenoids play in light-harvesting complexes?

2. Electronic Interactions and Energy Transfer

To analyze ultrafast EET it is important to understand the form and magnitude of the electronic interactions between chromophores, since they are a key component of the rate expression.^{30,31} In the condensed phase the time-dependent transition probability involves an entanglement between the electronic factors and the dynamics of chromophore–bath interactions (i.e., interactions of the type which effectuate homogeneous line broadening). Rate expressions for a (weakly-coupled) bichromophoric system are indicated in eqs 1. (Here

$$W = 2\text{Re}\left(\frac{-i}{\hbar}\right) |T_{\text{RP}}|^2 \sum_r \bar{P}(r) \int_0^\infty dt_1 \exp[i\omega_{\text{rp}} t_1 - g(t_1)] \quad (1a)$$

$$w = \frac{1}{c\hbar^2} |T_{\text{RP}}|^2 \bar{J} \quad (1b)$$

we use “chromophore” to denote any molecule or molecular component upon which electronic excitation may be localized.)

These equations are applicable in the nonadiabatic limit, although it is possible that in photosynthetic light-harvesting systems the electronic coupling is strong enough that this is not a good approximation. Nonetheless, eqs 1 clearly show the separation between electronic factors (T_{RP}) and the spectral overlap term (\bar{J}). $\bar{P}(r)$ denotes the initial level population of the reactant, R (with vibronic levels r), $g(t)$ is the line broadening function (familiar from analysis of non-linear optical phenomena³²) and T_{RP} is the electronic transfer matrix element which couples the reactant and product electronic configurations.

Equation 1b is adduced directly from the derivation of Förster, written in a form such that \bar{J} is the spectral overlap integral between area-normalized donor fluorescence, $f_R(\nu)$, and acceptor absorption, $a_P(\nu)$, spectra on a wavenumber scale: $\bar{J} = \int_0^\infty d\nu f_R(\nu) a_P(\nu)$. Mukamel and Rupasov³³ have shown how to account for “hot” energy transfer by expressing $f_R(\nu)$ as a time-dependent fluorescence line shape, which, at long times reduces to the Förster spectral overlap integral.

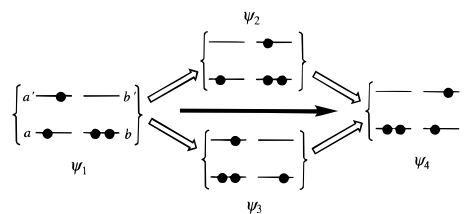


Figure 1. Localized molecular orbital (LMO) configurations interacted in the model described in ref 12 for the description of electronic coupling between a singlet or triplet open-shell excited state of a donor chromophore (A^*) and a closed-shell ground state acceptor (B). ψ_2 and ψ_3 are intermediate charge transfer configurations (cf. section 2).

Provided the coupling is weak, eq 1 applies to Förster¹ or Dexter² energy transfer, or to any case in between, since differentiation between these limits is determined entirely by the electronic coupling matrix element T_{RP} . If T_{RP} is simply a dipole–dipole interaction, then we are in the Förster limit (i.e., R^{-6} distance dependence for the rate); for triplet–triplet energy transfer we have the Dexter limit (i.e., exponential distance dependence of the rate); otherwise we have some combination of the two (i.e., $R^{-6} + \text{exponential} + \text{interference term}$ ³⁴).

A detailed theory for the electronic interactions, T_{RP} , has been developed recently.¹² It is based upon a model four-electron, four-orbital picture which contains the essence of the problem. It may readily be generalized to accommodate a larger active space and/or electron correlation effects and superexchange-mediated interactions.¹⁴ This interaction matrix element may be estimated from experiment, for example from absorption or circular dichroism spectra, etc., but the results can sometimes be ambiguous, especially in complex multichromophoric assemblies. Thus, in many instances, a quantum chemical estimation of the magnitude and origins of the electronic coupling is useful.

In ref 12 the energy transfer matrix element T_{RP} was obtained in terms of a model involving localized molecular orbitals (LMOs). In this picture various configurations are interacted; primarily those for which excitation is localized at a chromophore (which we write as $A^* \cdots B$ or $A \cdots B^*$, labeled ψ_1 and ψ_4 respectively, for chromophores A and B). This basic treatment is improved by adding further configurations (contributing to the coupling with smaller weight), such as the charge transfer configurations $A^+ \cdots B^-$ and $A^- \cdots B^+$ (ψ_2 and ψ_3). This is illustrated in Figure 1. Note that the ψ_i are *configuration wave functions* not *state wave functions*, and consequently they are not orthogonal.

The interaction between locally-excited singlet states (ψ_1 and ψ_4) has a primary contribution from the Coulombic interaction (often approximated as a dipole–dipole coupling between transition moments). For singlet–singlet and triplet–triplet energy transfer there are further interactions between these configurations which involve interchromophore orbital overlap: generic Dexter-type interactions. Explicitly they involve penetration interactions, which account for delocalization of electrons between chromophores and distortion of the electron density owing to interpenetration of their orbitals, and the Dexter integral itself (which has been found to be comparatively small in magnitude).¹³

The charge transfer (CT) configurations (ψ_2 and ψ_3) mediate additional interactions dependent upon interchromophore orbital overlap. (We emphasize that these configurations are unique to the LMO picture.) The electronic coupling due to this component of the overall interaction is the most significant, after the Coulombic interaction, and should not be ignored at separations where interchromophore orbital overlap effects may be important.

ψ_2 and ψ_3 promote energy transfer by mediating virtual electron transfer–hole transfer and *vice versa* superexchange; thus they are not accounted for in a two-level model. They account for a polarization resonance which delocalizes excitation energy. The charge transfer configurations are generally not localized because they are usually higher in energy than the locally excited states (otherwise one would have electron transfer rather than energy transfer). This interaction mechanism was posed intuitively by Closs et al. in a comparison of electron transfer and triplet–triplet energy transfer.³⁵ In the same spirit, a theoretical comparison was published recently.³⁶

A significant consequence of the charge transfer-mediated interactions (the through-configuration interaction) is that they affect also the ground to excited stationary state transition moments,^{15,37} in addition to the superradiance effect.³⁸ Hence analysis of the extent of delocalization of excitation using measurement oscillator strength or superradiance may be affected.

3. Calculating the Electronic Interactions

In this section the theory is summarized and its connection with an isomorphic molecular orbital (MO) treatment is demonstrated. The theory has been developed for excited states formed by single electron excitation from a closed-shell ground state. Application to closed-shell excited states such as the carotenoid 2^1A_g state is discussed in section 4.

Localized MO Configurations. The model has been formulated in terms of MOs localized on donor and acceptor chromophores (a, a', b and b'). To be consistent with the previous work^{12–14} we retain here the labeling of the donor HOMO/LUMO orbitals as a/a' and corresponding acceptor orbitals as b/b' . The theory of ref 12 was described in terms of the locally-excited (LE) configurations $\psi_1(A^*B)$ and $\psi_4(AB^*)$ and the charge-transfer (CT) configurations $\psi_2(A^+B^-)$ and $\psi_3(A^-B^+)$ between donor A and acceptor B chromophores. These configurations have been written in terms of antisymmetrized products of the LMOs (with a bar denoting that they accommodate an electron of β spin, otherwise containing an electron of α spin), according to eq 2,

$$\begin{aligned}\psi_1 &= N_1(|a\bar{a}'b\bar{b}| \pm |a'\bar{a}b\bar{b}|) \\ \psi_2 &= N_2(|a\bar{b}'b\bar{b}| \pm |b'\bar{a}b\bar{b}|) \\ \psi_3 &= N_3(|a\bar{a}b\bar{b}'| \pm |a\bar{a}a'\bar{b}|) \\ \psi_4 &= N_4(|a\bar{a}b\bar{b}'| \pm |a\bar{a}b'\bar{b}|)\end{aligned}\quad (2)$$

where the N_i are normalizing coefficients, and properly antisymmetrized wave functions are written as Slater determinants ($|\dots|$).

We shall use primarily symmetric sandwich-type dimer systems (as previously) in order to demonstrate further aspects of this theory. For the π -electrons of this type of dimer the only LMO overlap integrals which are nonzero are $S_{ab} \equiv \langle a|b \rangle$ and $S_{a'b'} \equiv \langle a'|b' \rangle$. (For a general dimer the $S_{a'b'}$ -type overlap-dependent terms enter via the normalization factors only.) The Slater determinants of each of the ψ_i are orthogonal. It is convenient here to define each Slater determinant in eq 2 as, for example $\hat{A}a\bar{a}'b\bar{b}$ with $\hat{A} = (4!)^{-1} \sum^P (-1)^P \hat{P}$. When this is done the Slater determinants are not normalized. Each of the normalization constants of eq 2 is then equal to $1/(2(1 - S_{ab}^2)^{1/2})$ for two electrons of the same spin. The orbital occupancies for ψ_1 to ψ_4 are displayed in Figure 1.

Dimer or Canonical MO Configurations. We now turn our attention to the configurations that arise from use of orthogonal canonical MOs (CMOs) for the donor–acceptor dimer and relate these configurations to the LMO configurations

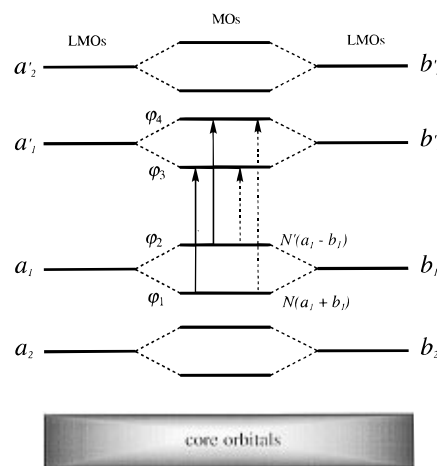


Figure 2. Illustration of the relationship between the active space localized MOs of donor and acceptor chromophores (a, b , etc.) and the corresponding dimer canonical MOs (ϕ_i), constructed as linear combinations of the LMOs. Core orbitals are those orbitals not included explicitly in the active space.

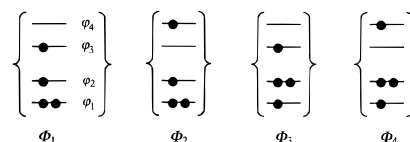


Figure 3. Canonical MO configurations formed from the dimer CMOs. Their correspondence with LMO configurations is established in eqs 4.

of eq 2 (cf. Figure 2). The advantages for a full MO treatment is that it is more easily undertaken, using a standard *ab initio* (or possibly semiempirical) package.

Since each of the a and b is orthogonal to a' and b' ; the CMOs for the dimer are those of eqs 3.

$$\phi_1 = (a + b)/(2 + 2S_{ab})^{1/2} \quad (3a)$$

$$\phi_2 = (a - b)/(2 - 2S_{ab})^{1/2} \quad (3b)$$

$$\phi_3 = (a' + b')/(2 + 2S_{a'b'})^{1/2} \quad (3c)$$

$$\phi_4 = (a' - b')/(2 - 2S_{a'b'})^{1/2} \quad (3d)$$

where S_{ab} is the overlap integral between LMOs a and b . These MOs may be used to construct the CMO configurations of eqs 4, whose orbital occupancies are displayed in Figure 3. Using the identities of the type $|\phi_1\phi_2\dots| = -|ab\dots|/(1 - S_{ab}^2)^{1/2}$, the Φ_i may be expressed as linear combinations of the ψ_i of eq 2, as indicated also in eqs 4.

$$\begin{aligned}{}^{1,3}\Phi_1 &= (|\phi_1\bar{\phi}_1\phi_2\bar{\phi}_3| \pm |\phi_1\bar{\phi}_1\phi_3\bar{\phi}_2|)/\sqrt{2} \\ &= K_1(\psi_1 + \psi_2 - \psi_3 - \psi_4)\end{aligned}\quad (4a)$$

$$\begin{aligned}{}^{1,3}\Phi_2 &= (|\phi_1\bar{\phi}_1\phi_2\bar{\phi}_4| \pm |\phi_1\bar{\phi}_1\phi_4\bar{\phi}_2|)/\sqrt{2} \\ &= K_2(\psi_1 - \psi_2 - \psi_3 + \psi_4)\end{aligned}\quad (4b)$$

$$\begin{aligned}{}^{1,3}\Phi_3 &= (|\phi_2\bar{\phi}_2\phi_1\bar{\phi}_3| \pm |\phi_2\bar{\phi}_2\phi_3\bar{\phi}_1|)/\sqrt{2} \\ &= K_3(\psi_1 + \psi_2 + \psi_3 + \psi_4)\end{aligned}\quad (4c)$$

$$\begin{aligned}{}^{1,3}\Phi_4 &= (|\phi_2\bar{\phi}_2\phi_1\bar{\phi}_4| \pm |\phi_2\bar{\phi}_2\phi_4\bar{\phi}_1|)/\sqrt{2} \\ &= K_4(\psi_1 - \psi_2 + \psi_3 - \psi_4)\end{aligned}\quad (4d)$$

where

$$\begin{aligned} K_1^{-1} &= -2[(1 + S_{ab})(1 + S_{a'b'})]^{1/2} \\ K_2^{-1} &= -2[(1 + S_{ab})(1 - S_{a'b'})]^{1/2} \\ K_3^{-1} &= -2[(1 - S_{ab})(1 + S_{a'b'})]^{1/2} \\ K_4^{-1} &= -2[(1 - S_{ab})(1 - S_{a'b'})]^{1/2} \end{aligned} \quad (5)$$

Hence, we adduce eqs 6, which represent the LMO configuration wave functions employed in the elucidation of T_{RP} in terms of the canonical molecular orbitals of the dimer.

$$\psi_1 = (\Phi_1/K_1 + \Phi_2/K_2 + \Phi_3/K_3 + \Phi_4/K_4)/4 \quad (6a)$$

$$\psi_2 = (\Phi_1/K_1 - \Phi_2/K_2 + \Phi_3/K_3 - \Phi_4/K_4)/4 \quad (6b)$$

$$\psi_3 = (-\Phi_1/K_1 - \Phi_2/K_2 + \Phi_3/K_3 + \Phi_4/K_4)/4 \quad (6c)$$

$$\psi_4 = (-\Phi_1/K_1 + \Phi_2/K_2 + \Phi_3/K_3 - \Phi_4/K_4)/4 \quad (6d)$$

Using these relationships, the LMO configuration Hamiltonian matrix elements $H_{ij}^{(m)} = \langle \psi_j | H | \psi_i \rangle$ and overlap integrals $S_{ij}^{(m)} = \langle \psi_j | \psi_i \rangle$ may be obtained once the dimer MO configuration matrix elements have been obtained (from, for example, a CAS-SCF calculation). In particular, using eqs 5 and 6, it is easy to deduce that $S_{12}^{(m)} = -S_{a'b'}$, $S_{13}^{(m)} = S_{ab}$ and $S_{14}^{(m)} = S_{ab}S_{a'b'}$, as were obtained directly from the ψ_1 to ψ_4 in ref 12.

Now, the electronic coupling, T_{RP} , is determined by solving the secular equations of eq 7 for energy relative to that of the A*B configuration, with $T_{IJ} = H_{IJ} - S_{IJ}H_{11}$ and $\epsilon = E - H_{11}$.

$$\sum_j (T_{IJ} - \epsilon S_{IJ}) C_j = 0 \quad (7)$$

The reactant and product configurations may be defined in terms of the active space configurations as indicated in eqs 8a for the four-electron, four-orbital model and eqs 8b for a general model.

$$\begin{aligned} \Psi_R &= c_1\psi_1 + c_2\psi_2 + c_3\psi_3 \\ &= N_R(\psi_1 + \lambda_R\psi_2 + \mu_R\psi_3) \\ \Psi_P &= d_4\psi_4 + d_2\psi_2 + d_3\psi_3 \\ &= N_P(\psi_4 + \mu_P\psi_2 + \lambda_P\psi_3) \end{aligned} \quad (8a)$$

$$\begin{aligned} \Psi_R &= (c_1\psi_1 + c_1\psi_{1'} + \dots) + (c_2\psi_2 + c_2\psi_{2'} + \dots) + \\ &\quad (c_3\psi_3 + c_3\psi_{3'} + \dots) + \dots \end{aligned} \quad (8b)$$

$$\begin{aligned} \Psi_P &= (d_4\psi_4 + d_4\psi_{4'} + \dots) + (d_2\psi_2 + d_2\psi_{2'} + \dots) + \\ &\quad (d_3\psi_3 + d_3\psi_{3'} + \dots) + \dots \end{aligned} \quad (8b)$$

The more general formulation given in eq 8b includes explicit consideration of a larger active space than that used in the four-electron, four-orbital picture. Hence, terms in parentheses include the various singly-excited configurations that contribute to the basic A*B, A⁺B⁻, A⁻B⁺, and AB* configurations (as depicted in Figure 2). Similarly, doubly-excited (and higher order) configurations may be included. The effect of CI may be considerable, as was ascertained recently.¹³

The coefficients relate to the λ and μ defined earlier ($\lambda_R \equiv c_2/c_1$, $\mu_R \equiv c_3/c_1$, etc.). In general they cannot be determined from the full CAS-SCF treatment. They are found by solving eqs 7 for each of the Ψ_R and Ψ_P , that is, where the locally excited final and initial states respectively are omitted from the

secular equations. The matrix elements are determined from transformed CAS-SCF matrix elements between the various configurations. Using eqs 8a we write the interaction in terms of the LMO matrix elements as eqs 9

$$\begin{aligned} T_{RP} &= c_1d_4T_{14} + \{c_1d_3T_{13} + c_2d_4T_{24} + c_3d_3A_{13}\} + \\ &\quad \{c_1d_2T_{12} + c_3d_4T_{34} + c_2d_2A_{12}\} + (c_2d_3 + c_3d_2)T_{23} \end{aligned} \quad (9a)$$

$$\begin{aligned} &\approx c_1d_4T_{14} + c_2d_4T_{24} + c_3d_4T_{34} \\ &\equiv c_1d_4(T_{14} + \lambda T_{24} + \mu T_{34}) \end{aligned} \quad (9b)$$

in which $T_{ij} = H_{ij}^{(m)} - S_{ij}^{(m)}H_{11}^{(m)}$ and $A_{ij} = H_{ij}^{(m)} - H_{ii}^{(m)}$.

For the sandwich dimer configuration studied previously, $\lambda_R = \lambda_P = \lambda$ and $\mu_R = \mu_P = \mu$ in eq 8a. The λ and μ may then be calculated from the C_i coefficients that are obtained from dimer MO-CI calculations as follows:

$$\begin{aligned} \Psi_- &= C_1\Phi_1 + C_4\Phi_4 \\ &= (C_1K_1 + C_4K_4)(\psi_1 - \psi_4) + (C_1K_1 - C_4K_4)(\psi_2 - \psi_3) \\ &\equiv \Psi_R - \Psi_P \\ &= N\{\psi_1 - \psi_4 + (\lambda - \mu)(\psi_2 - \psi_3)\} \end{aligned} \quad (10a)$$

$$\begin{aligned} \Psi_+ &= C_2\Phi_2 + C_3\Phi_3 \\ &= (C_2K_2 + C_3K_3)(\psi_1 + \psi_4) + (C_3K_3 - C_2K_2)(\psi_2 + \psi_3) \\ &\equiv \Psi_R + \Psi_P \\ &= N\{\psi_1 + \psi_4 + (\lambda + \mu)(\psi_2 + \psi_3)\} \end{aligned} \quad (10b)$$

Alternatively, for small overlap between ψ_i and ψ_j , the λ and μ are given approximately by $-T_{12}/A_{12}$ and $-T_{13}/A_{13}$, respectively. The T_{ij} and A_{ij} may then be obtained from dimer MO-CI calculations via the use of eq 6.

Relationship to Steady State Spectra. It is useful to relate the theory established in ref 12 to the electronic absorption spectrum of a dimer formed between two identical molecules. In this case the stationary states of the system are given as linear combinations of the reactant and product wavefunctions, eq 11.

$$\begin{aligned} \Psi_+ &= (\Psi_R + \Psi_P)/(2 + 2S_{RP})^{1/2} \\ \Psi_- &= (\Psi_R - \Psi_P)/(2 - 2S_{RP})^{1/2} \end{aligned} \quad (11)$$

From consideration of the energies of these states, it follows that half the energy difference between these states (i.e., half the “splitting”) is given as

$$(E_- - E_+)/2 \equiv \Delta = [-H_{RP} + 1/2(H_{RR} + H_{PP})S_{RP}]/[1 - S_{RP}^2] \quad (12a)$$

$$\begin{aligned} &\approx -H_{RP} + 1/2(H_{11} + H_{44})S_{RP} \\ &= -T_{RP} \end{aligned} \quad (12b)$$

where eq 12b is accurate to second order to interchromophore orbital overlap (see eq 6 of ref 12). (The same result is not obtained for a heterodimer.) Although this result appears obvious, it is important to establish that Δ determines the total electronic coupling, not just the “direct” coupling T_{14} .

Similarly, we may consider the sum of these energies and therefore elucidate the origin of the stabilization of the dimer states relative to the monomer state. It is found that, in the

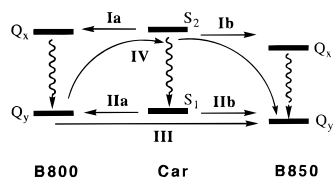


Figure 4. A scheme depicting the energy transfer pathways between carotenoid (S_1 and S_2 states), B800 and B850 (Q_x and Q_y bands) chromophores in LH2. Discussion of the electronic couplings for each type of pathway is given in sections 4 and 6.

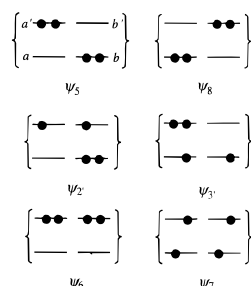


Figure 5. Additional LMO configurations used in section 4 for the investigation of Car-Car and Car-Bchl electronic couplings involving the Car S_1 state. ψ_2 , and ψ_3 , are the charge transfer configurations, and it is found that the primary configurations are the doubly-excited configurations, ψ_5 , ψ_7 , and ψ_8 .

simple four-electron, four-orbital model, this stabilization is due primarily to interaction between the LE and CT states, eq 13,

$$E_+ + E_- = H_{11} + H_{44} + E_{\text{int}}^{(1)} - 4E_{\text{int}}^{(2)} \quad (13)$$

where $E_{\text{int}}^{(1)}$ collects polarization interactions such as $\lambda^2 T_{12}$, and $E_{\text{int}}^{(2)}$ is the through-configuration interaction.¹² These interactions act to red-shift the dimer electronic absorption bands and to alter the transition oscillator strength, and the effects may often be significant.^{15,36}

4. Carotenoids and Energy Transfer

There has been much speculation regarding the mechanism of excitation energy transfer between carotenoids and chlorophylls^{29,39–44} because of the forbidden ground (S_0) to first excited state (S_1) transition of carotenoids (similar to that of polyenes).⁴⁵ This lowest carotenoid (Car) electronic state arises primarily from a double excitation from HOMO to LUMO orbitals and is therefore electric dipole forbidden (the state product is totally symmetric). In a notation derived from C_{2h} point group polyenes it is labeled 2^1A_g , while the ground state is denoted 1^1A_g . The second electronic excited state (S_2) is observed in absorption spectra and arises primarily from a single excitation from HOMO to LUMO and is labeled the 1^1B_u state.^{39,46} The $S_2 \leftarrow S_0$ transition is dipole-allowed.

A number of studies of energy transfer between carotenoids and Bchl in bacterial light-harvesting complexes have been reported.^{39,40,47,48} A scheme depicting the energy levels and types of coupling may be deduced from these results and is shown in Figure 4 (and will be discussed further in section 6). It is accepted that the Förster mechanism cannot promote Car(2^1A_g) \rightarrow Bchl(Q_y) energy transfer (pathways II), primarily because the carotenoid $2^1A_g \rightarrow 1^1A_g$ transition has a zero dipole transition moment. Thus it has been postulated that a “Dexter” mechanism mediates the Car(2^1A_g) \rightarrow Bchl(Q_y) energy transfer which has been observed for several bacterial light-harvesting antennae.^{28,47} The Förster mechanism may, however, mediate Car(1^1B_u) \rightarrow Bchl(Q_x) energy transfer (pathways I) if it can compete with internal conversion. The possibility of Car(1^1B_u) \rightarrow Bchl(Q_y) energy transfer, for which the electronic coupling

should similarly be large, is remote owing to the poor spectral overlap factor (cf. eq 1). It is unlikely that carotenoid-carotenoid energy transfer occurs in LH2,⁴⁷ although it may turn out to be necessary to consider the coupling between the carotenoid identified originally in *Rps. acidophila* and that identified more recently.⁴⁹

In this section we investigate the origin of electronic coupling for systems involving carotenoids (or polyenes). It is demonstrated that the primary form of this coupling is quite different from the “normal” case of singlet-singlet energy transfer discussed in sections 2 and 3. To elucidate the form of the electronic coupling mediating Car-Car or Car-Bchl energy transfer we consider, in addition to the configurations of eq 2, the doubly-excited (normalized) singlet configurations of eq 14,

$$^1\psi_5 = |a'\bar{a}bb|$$

$$^1\psi_7 \approx (|a\bar{a}b\bar{b}| + |a'\bar{a}b\bar{b}| + |a\bar{a}b'b| + |a'\bar{a}b'b|)/2 \quad (14)$$

$$^1\psi_8 = |a\bar{a}b\bar{b}'|$$

The $^1\psi_5$ and $^1\psi_8$ are the initial and final locally doubly-excited carotenoid configurations ($A^{**}B$ and AB^{**}), whereas $^1\psi_7$ involves a single excitation on each chromophore with opposed spins for the a and a' electrons and for the b and b' electrons [$A^*(S=0)B^*(S=0)$]. The treatment may be elaborated further by the inclusion of the additional charge transfer and correlated configurations of eqs 15, although it shall be demonstrated that

$$^1\psi_2 \approx (|a'\bar{b}bb| + |b'\bar{a}bb|)/\sqrt{2}$$

$$^1\psi_3 \approx (|a'\bar{b}aa| + |b'\bar{a}aa|)/\sqrt{2} \quad (15a)$$

$$^1\psi_0 = |a\bar{a}bb|$$

$$^1\psi_6 = |a'\bar{a}b\bar{b}'| \quad (15b)$$

they are not associated with the primary interaction at intermediate separations, which is independent of interchromophore orbital overlap.

We begin by considering the coupling for Car-Car energy transfer such that 2^1A_g state excitation is exchanged (i.e. energy transfer originating from the Car S_1 state). We then examine the exchange of carotenoid 2^1A_g state excitation with Bchl 1^1Q_y state excitation (i.e., pathways II of Figure 4). We aim to establish here the origins and distance dependences of these interactions.

Carotenoid-Carotenoid Electronic Coupling. As will be demonstrated in this section, the case of Car(2^1A_g)-Car(2^1A_g) energy transfer is quite different from the normal singlet-singlet energy transfer discussed in section 2. It is not promoted by a dipole-dipole coupling, since the $2^1A_g \leftarrow 1^1A_g$ transition is electric dipole forbidden; however, an electric quadrupole or magnetic dipole interaction may mediate virtual photon exchange in the spirit of the Förster mechanism.³ The complete electronic coupling interaction is derived here, where it is found that the leading interchromophore orbital overlap-dependent interactions are very different to the Dexter interaction, both in origin and distance dependence.

In order to treat properly the interaction mediating energy transfer between a 2^1A_g excited state carotenoid (or polyene) and a nearby ground (1^1A_g) state carotenoid, careful account must be taken of electron correlation effects involving double excitations from the reactant and product reference configurations (ψ_5 and ψ_8 , respectively). We ignore here the carotenoid CT configurations ψ_2 and ψ_3 of eq 15b since their contribution

can be shown to be negligibly small. To begin, we write the correlated reactant and product configurations as in eq 16, where

$$\begin{aligned}\Psi_R &= N_R(\psi_5 = \alpha_R\psi_6 + \beta_R\psi_0 + v_R\psi_7) \\ \Psi_P &= N_P(\psi_8 + \alpha_P\psi_6 + \beta_P\psi_0 + v_P\psi_7)\end{aligned}\quad (16)$$

the N are normalizing constants and the α , β , and v are mixing coefficients. The $\alpha\psi_6$ admits a double excitation correlation correction to the ground state LMO wave function, while the $\beta\psi_0$ adds an analogous correction to the excited state LMO wave function. When this approach is pursued, it is found that cancellations arise owing to approximate degeneracies between the energy gaps A_{56} and $-A_{50}$, suggesting that to a reasonable approximation the coupling is not mediated by these configurations at all. Hence, to present a clearer derivation, we set α and β to zero from the start—thus we rewrite eq 16 as eq 17

$$\begin{aligned}\Psi_R &= N_R(\psi_5 + v_R\psi_7) \\ \Psi_P &= N_P(\psi_8 + v_P\psi_7)\end{aligned}\quad (17)$$

with $N_R = (1 + v_RS_{57} + v_R^2)^{-1/2}$ and $N_P = (1 + v_PS_{87} + v_P^2)^{-1/2}$. Then, assuming the v are small, so that $v_R \approx -H_{57}/A_{57}$ and $v_P \approx -H_{78}/A_{87}$, with energy gaps defined as $A_{ij} = H_{ij} - H_{ii}$, we obtain eq 18;

$$\begin{aligned}T_{RP} &= H_{RP} - S_{RP}H_{55} \\ &= N_RN_P(T_{58} - T_{57}T_{78}/A_{57})\end{aligned}\quad (18)$$

Each of the T_{57} and T_{78} is formally equivalent to the T_{14} considered previously (cf. refs 12–14). Hence, each of these matrix elements may be expressed as $2J - Z - P$, in which J and Z are the Coulomb and Dexter exchange integrals, and P is the sum of integrals that provide a penetration contribution to the T_{ij} matrix element. For small overlap between the chromophore orbitals, the Coulombic integral usually provides the dominant contribution to the matrix element. When this is the case, we have $T_{57} \approx 2J^{(A)}$ and $T_{78} \approx 2J^{(B)}$, where $2J$ is the Coulombic integral ($a'a|bb'$) referring to the $1^1B_u \leftrightarrow 1^1A_g$ transition of A or B as indicated (i.e., primarily a dipole–dipole interaction). $A_{57} \approx J_0^{(A)} + J_0^{(B)}$ is the energy gap between configurations ψ_5 and ψ_7 (J_0 is approximately equal to half the splitting between the 1^1B_u and 1^3B_u states of A or B). For the direct interaction between configurations ψ_5 and ψ_8 we find that $T_{58} \approx -2S_{ab}S_{a'b'}J$, where $S_{ij} = \langle j|i \rangle$ is an orbital overlap integral.

Further to the above treatment, we need to consider the Coulombic coupling between transition densities.^{3,50–52} In our primary orbital treatment $u^{\text{Coul}} = 2\langle a'\bar{a}'b\bar{b}'|r_{ij}^{-1}|a\bar{a}b'\bar{b}' \rangle$ is zero because of the orthogonality between a and a' and b and b' . However, if a quantum electrodynamical treatment of this interaction is adopted,^{3,50} it is seen that u^{Coul} is not zero (as is also found by accurate CMO calculation), since a nonzero transition moment may be associated with each of the deexcitation and excitation transitions (involving odd rank magnetic transition moment tensors and even rank electric transition moment tensors). In the present case the interaction is mediated primarily via the coupling between magnetic dipole and electric quadrupole transition moments.

Hence we deduce that the electronic coupling between two carotenoids is given by eq 19

$$T_{RP} \approx u^{\text{Coul}} - 4J^2/A_{57} - 2S_{ab}S_{a'b'}J \quad (19)$$

It is evident, therefore, that the energy transfer mechanism is quite complex but contains reasonably long-range interaction terms. Dispersion-type interactions, which have an R^{-6} distance dependence, should provide a significant, if not the primary, contribution to the coupling, via J^2/A_{57} . u^{Coul} should contribute to the coupling, with magnetic dipole–dipole (attenuated as R^{-3}), magnetic dipole–electric quadrupole (R^{-4}), and electric quadrupole–quadrupole (R^{-5}) terms dominating.^{29,50} The final term of eq 19 contains an explicit overlap dependence and will therefore be small (cf. ref 13). In fact, using the integrals obtained for the ethene sandwich dimer,¹³ it is seen that $u^{\text{disp}} = -0.0143$ eV compared to $-2S_{ab}S_{a'b'}J = -0.000\,012$ eV. Hence we have eq 20,

$$T_{RP} \approx u^{\text{Coul}} + u^{\text{disp}} \quad (20)$$

where the appropriate form of u^{Coul} is discussed elsewhere⁵⁰ and the dispersion interaction, u^{disp} , has a form similar to the London formula,⁵¹ as can be seen from related studies.^{52–54} Estimation of typical magnitudes of this coupling is discussed in section 6.

Carotenoid–Bchl Electronic Coupling. The coupling of the $2^1A_g \rightarrow 1^1A_g$ carotenoid transition to the Bchl 1^1Q_y transition (pathways II of Figure 4) is another case which requires careful consideration. To ascertain the form of the coupling we begin with reactant and product wave functions analogous to those of ref 12, eq 21, where the λ and μ are small mixing coefficients (cf. eq 8a of section 3). We then include an additional configuration, ψ_7 (as for carotenoid–carotenoid coupling). Correlated doubly-excited configurations are not included.

$$\begin{aligned}\Psi_R &= N_R(\psi_5 + \lambda_R\psi_{2'} + \mu_R\psi_{3'} + v_R\psi_7) \\ \Psi_P &= N_P(\psi_4 + \mu_P\psi_{2'} + \lambda_P\psi_{3'} + v_P\psi_7)\end{aligned}\quad (21)$$

Assuming μ , λ , v_R , and v_P are small, we adduce eq 22:

$$T_{RP} \approx T_{54} - T_{52'}T_{2'4}/A_{52'} - T_{53'}T_{3'4}/A_{53'} - T_{57}T_{74}/A_{57} \quad (22)$$

In the spirit of ref 12, the matrix elements may be evaluated explicitly from the configuration wave functions given in eqs 14–15. Those involving ψ_5 , ψ_7 , ψ_4 , and $\psi_{2'}$, are collected in eqs 23. The $T_{53'}$ and $T_{3'4}$ have a form related to $T_{52'}$ and $T_{53'}$.

$$\begin{aligned}T_{54} &= -\sqrt{2}\{(a'a|b'b')S_{ab} + (a'a|ab)S_{a'b'}\} \\ T_{52'} &= \sqrt{2}\{h_{a'b'} + (a'b'|a'a') + (a'b'|bb) - \\ &\quad S_{a'b'}[h_{aa} + (aa|bb) + (aa|a'a')] + (a'b'|bb) - S_{a'b'}(aa|bb)\} \\ &= \sqrt{2}(\tilde{B}' + \tilde{Q}') \\ T_{2'4} &= \sqrt{2}(a'a|bb')S_{ab'} \\ &\equiv \sqrt{2}JS_{ab'} \\ T_{57} &\approx 2J \\ T_{74} &= \sqrt{2}\{(aa|aa') + (bb|aa') + (b'b'|aa')\}\end{aligned}\quad (23)$$

The notation employed previously has been used here. \tilde{B}' and \tilde{Q}' denote penetration and exchange-type terms, closely related to the B' and Q' in eqs 19–21 of ref 14. Again, note that the Coulomb integral ($2J$) is that between the carotenoid 1^1B_u state and the Bchl Q_y . Owing to orbital symmetry, T_{74} is equal to zero in symmetrical systems (e.g., sandwich dimers). However, with a lowering of symmetry, it is not zero, in which

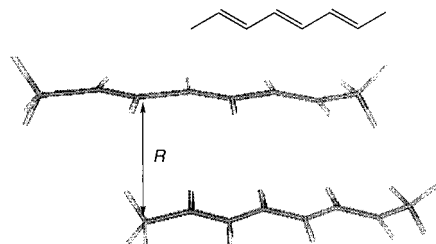


Figure 6. Octatriene dimer configuration used for the model calculations reported in section 5. Note that R is a "nearest approach" separation, not the center-to-center separation. The *all-trans*-octatriene (OCT3) is depicted also.

case the $-T_{57}T_{74}/A_{57}$ term, which is not overlap-dependent, should be substantially larger than the remaining, overlap-dependent, terms of eq 22. Consequently, the primary contributor to the T_{RP} for Car-Bchl $S_1 \rightarrow S_1$ energy transfer should be proportional to the product of dipole-dipole and polarization interactions.

As discussed in the treatment of carotenoid-carotenoid coupling, above, we should also consider u^{Coul} , the Coulombic interaction between the Car $2^1A_g \rightarrow 1^1A_g$ and Bchl $S_0 \rightarrow 1^1Q_y$ transitions, since it is not recovered from our primary orbital treatment. These considerations yield the conclusion that the total electronic coupling between Car(2^1A_g) and Bchl is given by eq 24, where u^{Coul} is the Coulombic interaction, involving

$$T_{RP} \approx u^{\text{Coul}} + u^{\text{pol}} + u^{\text{ic}} \quad (24)$$

primarily Car (magnetic dipole, electric quadrupole)-Bchl (electric dipole) coupling (R^{-2} , R^{-4} distance dependences),^{29,50} and u^{ic} denotes an interaction similar to the through-configuration interaction¹² which is dependent upon interchromophore orbital overlap. u^{pol} is a polarization-type interaction;⁵⁴ actually involving a Coulombic coupling together with a dynamic polarization coupling (which probably has an R^{-5} distance dependence, although this is currently being investigated). The distance dependence of eq 24 is examined further in section 6.

5. Calculations of Carotenoid/Polyene Excited States and Interactions

Electronic Coupling in a Polyene Dimer. The results of the previous section indicate that the form of the electronic coupling between an S_1 (2^1A_g state) carotenoid and a ground state carotenoid should be complex and largely independent of orbital overlap. In order to obtain a clearer picture of this interaction we report here the results of some model calculations of such an interaction.

We have undertaken some complete active space SCF (CAS-SCF) calculations^{56,57} on a model polyene, 2,4,6-octatriene (OCT3), using Gaussian 94.⁵⁸ The *all-trans* geometry of the molecule was determined by geometry optimization at the HF/STO-3G level (constraining the geometry to the C_{2h} point group). A staggered, overlapped geometry was chosen for the dimer with various (closest approach) separations between the two monomers (Figure 6). It should be emphasized at the outset that the results presented here are meant to be illustrative, not quantitative.

CAS-SCF calculations of the ground and excited singlet states were carried out using STO-3G, 3-21G, 3-21G*, and 6-31G basis sets. The active space for the monomer consisted of four electrons and four orbitals (of b_g and a_u symmetry). The corresponding orbitals of the dimer made up an active space of eight electrons and eight orbitals. For the dimer, a state average was carried out over the two excited states corresponding to the split OCT3, S_1 state. The CAS-SCF method is well-suited

for these calculations since it may account properly for CI/correlation effects within a set of active space orbitals (see ref 59).

The results of the calculations at the CAS-SCF/3-21G* level of monomer ground and lowest excited state, together with the corresponding dimer states, are collected in Table 1. The excited states of the dimer represent a splitting of the monomer 2^1A_g state owing to the interaction (approximately $2T_{RP}$, cf. eq 12). We label these states 2^1A_{g+} and 2^1A_{g-} , as in Ψ_+ and Ψ_- . The dominant configurations contributing to each wave function, together with their coefficients and the spin orbitals from which each configuration wave function may be constructed are provided.

The monomer calculation (3-21G* basis set) determined the S_0-S_1 vertical gap of OCT3 to be 7.24 eV. This calculated vertical excitation energy would be lowered by using a larger basis set and including $\sigma-\pi$ dynamic correlation effects in our calculations (cf. ref 59). Experimentally, the 0-0 $2^1A_g \leftarrow 1^1A_g$ excitation energy of the *all-trans* isomer of octatriene has been determined using resonance-enhanced multiphoton absorption under jet-cooled conditions to be 4.25 eV.⁶⁰ Because this is the 0-0 excitation energy, it cannot be compared directly with our calculated vertical excitation energy, which is necessarily larger. A better gauge, perhaps, is to compare our results for *all-trans*-octatriene with the CAS-SCF calculations of the excited states of *all-trans*-1,3,5,7-octatetraene reported by Serrano-Andres et al.⁵⁹ They determine the $2^1A_g \leftarrow 1^1A_g$ vertical excitation energy (for their *four* double bond polyene) to be 5.23 eV at the CAS-SCF level (11 orbital active space) and 4.38 eV with addition of some $\sigma-\pi$ dynamic correlation correction. As in previous studies,^{11,13,15,36} the purpose of these calculations is to determine splittings of the excited state and to examine the distance dependence of the coupling, not to quantify the excitation energies.

In Table 2 the results of calculations with a range of basis sets for 2,4,6-octatriene dimers of various separations are summarized. T_{RP} for each calculation is estimated by taking half the splitting of the 2^1A_g $\{[E(2^1A_{g-}) - E(2^1A_{g+})]/2\}$ state (eq 12). Included for comparison are triplet-triplet couplings for identical dimers, calculated using the CI singles method. The attenuations of the calculated couplings with separation are shown in Figure 7. The triplet-triplet coupling primarily involves interactions which depend upon interchromophore orbital overlap, which cause the strong, approximately exponential, diminution with increasing separation (the magnitude of which is very basis set dependent). The nonexponential distance dependence of the OCT3 S_1-S_1 indication, together with its weak attenuation and small magnitude at close separations, indicates the coupling is not primarily due to interchromophore orbital overlap-dependent interactions. The basis set dependence of this coupling may originate from, effectively, a reduction in calculated transition moment (i.e., bringing it closer to experimental observation) with better basis set, which in turn decreases the magnitude of u^{disp} .

Thus, as anticipated by the theory established in section 4, the calculated interaction is found to be (i) small in comparison to the overlap-dependent triplet-triplet interaction at close separations; (ii) small in comparison to a dipole-dipole interaction arising from the integral J for the dimer (i.e., the 1^1B_u coupling, not shown) at all separations; and (iii) quite weakly distance-dependent at larger separations.

The dimer wave functions may be interpreted by transforming the dimer CMO configurations into corresponding dimer LMO configurations, as discussed in section 3. Such an analysis reveals that the $(^{**})$ and $(^{*},^{*})$ dimer configurations consist of the various possible doubly-excited LMO configurations such

TABLE 1: Summary of the all-trans-Octatriene Dimer Calculations (CAS-SCF/3-21G*) with a 4 Å Separation of the Dimer^a

(0)	(1m) {1122}	(1d) {11223344}
(**)	(3m) {11}{33}	(14d) {112233}{66}
	(9m) {22}{33}	
	(11m) {11}{44}	
	(16m) {22}{44}	
(*)	(4m) {221}{3}	(10d) {1122334}{7}
	(5m) {112}{4}	(17d) {1133442}{6}
(*,*)	(10m) {12}{34}	(13d) {112234}{56}
	(12m) {12}{34}	(18d) {112234}{56}
		(63d) {114423}{57}
		(72d) {113324}{67}
		(165d) {223314}{68}

	monomer			dimer	
	energy	coefficients (Nm)		energy	coefficients (Nd)
1A _g	-308.20590	(1) 0.925 (0) (10) 0.206 (*,*) (4) -0.185 (*) (5) -0.155 (*) (3) -0.150 (**)	1A _g	-616.42315	(1) 0.810 (0) (17) 0.308 (*) (72) 0.220 (*,*) (10) 0.218 (*) (14) -0.173 (**)
2A _g	-307.93980	(3) 0.605 (**) (4) -0.498 (*) (5) -0.432 (*) (9) -0.228 (**) (11) -0.209 (**) (12) 0.204 (*,*) (16) 0.162 (**)	2A _{g+}	-616.17047	(13) 0.720 (*,*) (18) 0.421 (*,*) (165) 0.232 (*,*) (63) -0.207 (*,*) (14) 0.505 (**)
			2A _{g-}	-616.16975	(17) 0.479 (*) (10) 0.418 (*) (1) -0.250 (0) (72) 0.247 (*,*)

^a Energies are quoted in au. The configurations involving the eight active space molecular orbitals (four HOMOs and four LUMOs), 1 to 8, of the dimer are written explicitly below, (Nd), (where a barred orbital contains an electron of β spin). Similarly, those corresponding to the monomer calculation, 1 to 4, are listed also, (Nm). (N.B. Orbitals 1 to 4 of the monomer do not correspond to 1 to 4 of the dimer.) They are denoted either as the reference configuration (0), a double excitation (**), a single excitation (*) or a pair of single excitations (*,*).

TABLE 2: Distance (*R*) and Basis Set Dependences of the Octatriene 2^1A_g (S_1) State and 1^3B_u (T_1) State Electronic Couplings, $^1T_{RP}$ and $^3T_{RP}$, Determined by the CAS-SCF and CIS Methods, Respectively^a

	<i>R</i> , Å	<i>E</i> ₀ , au	ΔE^{dim} , eV	$^1T_{RP}$, cm ⁻¹	$^3T_{RP}$, cm ⁻¹
STO-3G	4.0	-612.430 66	7.7607	529	11
			7.8919		
3-21G	4.0	-616.423 20	6.8772	77	96
			6.8962		
3-21G*	3.5	-616.415 70	6.7482	243	460
			6.8083		
	4.0	-616.42 15	6.8748	79	96
			6.8954		
	4.5	-616.424 08	6.9028	48	15
			6.9147		
	5.0	-616.423 95	6.9058	40	2
			6.9156		
	5.5	-616.423 89	6.9039	36	0
			6.9128		
	6.0	-616.424 04	6.9052	36	0
			6.9142		
6-31G	4.0	-619.637 19	6.7760	41	103
			6.7860		

^a *E*₀ is the energy of the S_0 state, and ΔE^{dim} are the vertical excitation energies of the two dimer S_1 states (using the CAS-SCF method).

as ψ_5 , ψ_8 , and ψ_7 , while the (*) configurations consist of the singly-excited LMO configurations such as ψ_1 , ψ_2 , ψ_3 , ψ_4 , etc. This suggests that the electronic coupling may consist of, primarily, the mechanism proposed in the section 4 together with some contribution from a single excitation mechanism (section 2). This is in accord with the results for the 2^1A_g state of the monomer, indicating that this state consists mainly of doubly-excited configurations within the active space; however, there is a significant contribution from singly-excited configurations.

Rhodopin Glucoside in LH2. The calculations reported above and previously^{13,15} are for small model systems only. It

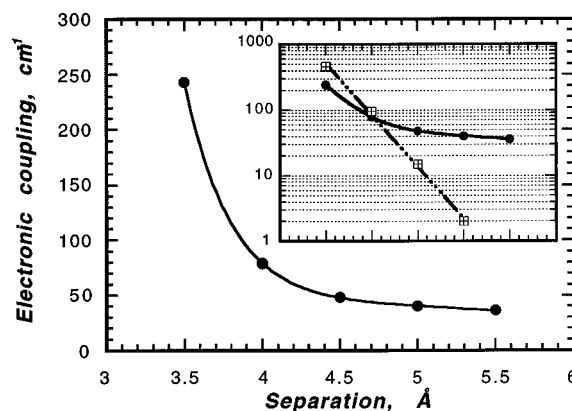


Figure 7. S_1 state coupling for various OCT3 separations, *R*, calculated using the CAS-SCF/3-21G* method. The inset compares this coupling with the triplet-triplet interaction, determined using the CIS/3-21G* method. It is evident that the calculated interaction is (i) small in comparison to the overlap-dependent triplet-triplet interaction at close separations; (ii) small in comparison to a dipole-dipole interaction (see text) at all separations; and (iii) quite weakly distance-dependent at larger separations.

is important to ascertain whether reliable *ab initio* calculations based on the theory described in the present work can be applied to large biological systems. The main obstacle here is that it is difficult enough to determine accurately an *ab initio* wave function for the S_1 state of a small model polyene, but a large carotenoid is an untried problem of immense complexity. At the present stage it makes sense to develop further the empirical expressions eqs 20 and 24 to quantify couplings involving the carotenoid S_1 state. In this regard it is seen from the CAS-SCF studies that, even for a small model compound, consideration of only singly and doubly excited configurations in the LMO theory is a gross simplification. In addition, it was found, for example, that singly-excited configurations provide a

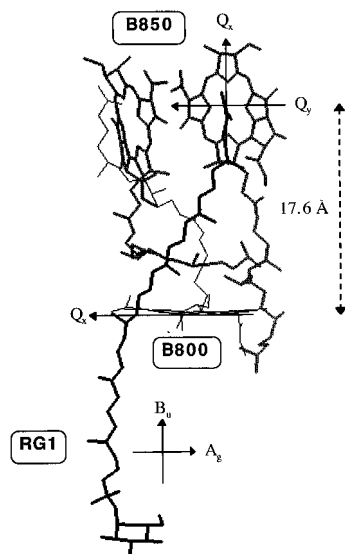


Figure 8. Depiction of the arrangement of the rhodopin glucoside, B800 Bchl *a* and B850 Bchl *a* dimer in LH2, together with their respective transition moments, using the coordinates of McDermott et al.¹⁶

significant contribution to the monomer S_1 state wave function, which will have a significant bearing on the energy transfer mechanism.

We have begun to undertake an investigation of the coupling between B800 and B850 Bchl *a* chromophores of LH2. The study aims to compare the coupling pathways III and IV of Figure 4, that is, direct versus superexchange coupling. Here we can circumvent the problem of determining the carotenoid S_1 state by assuming that the primary contribution to the superexchange interaction is mediated via the carotenoid S_2 state. Hence, we anticipate that the CI singles (CIS) level of theory will be sufficient, provided that the S_2 state of rhodopin glucoside (rg1) is adequately described. The structure of rg1 was taken from the coordinates of McDermott et al.¹⁶ Hydrogens were added and geometry-optimized at the MNDO level of theory while keeping the heavy atoms fixed. An initial CIS/3-21G calculation gives the vertical $S_2 \leftarrow S_0$ excitation as 2.35 eV, in close agreement with experiment,^{16b} suggesting that this approach may be reasonable.

6. Discussion: Role of Carotenoids in LH2

Carotenoids have been identified in photosynthetic reaction centers and light-harvesting membranes. They are involved in light harvesting, absorbing in the blue-green spectral region, and transferring this energy into the Bchl *a*-based antenna systems.⁴⁴ They also play an important photoprotective role by dissipating triplet states which could otherwise lead to damage from singlet oxygen. It is likely that they play an additional, structural role.

The crystal structure of the LH2 complex from the photosynthetic bacteria *Rhodospseudomonas acidophila* strain 10050 provides valuable structural information on the arrangement of B800 and B850 Bchl *a* aggregate rings and the carotenoids.¹⁶ The π -electron system of the carotenoid rhodopin glucoside is seen to reside in the hydrophobic protein domain and appears to be in van der Waals contact with both Bchl *a* antenna rings. The arrangement is depicted in Figure 8. Recently, a second carotenoid, lying on the other side of the Bchl *a* rings and approximately parallel to the first carotenoid, has been identified,⁴⁹ but not completely resolved.

The resolved carotenoids are distributed around the LH2 membrane with approximately 21 Å separations. The investigation of the form and magnitude of carotenoid–carotenoid

coupling given in sections 4 and 5 supports the suggestion of Andersson et al. that the coupling between carotenoids should be negligible for all intents and purposes. In the bacterial light-harvesting complex, light absorbed by the carotenoids is transferred via singlet–singlet interactions to B800 and B850 Bchl *a* chromophores in the ratio 25% to 75%.^{47,61,62} A photoregulatory role involving Bchl to carotenoid energy transfer may also occur, at least in green plant photosynthetic systems.^{39,63}

Experimental observations of carotenoid to Bchl *a* energy transfer reveal that transfer to B800 and B850 antennae is rapid and efficient.^{47,62,64,65} It has been suggested that most of the energy transfer occurs via the channels I of Figure 4 (i.e., $S_2 \rightarrow Q_x$).^{47,66} The coupling between carotenoid and Bchl is strong for this channel since it involves a dipole–dipole Coulombic interaction and the “normal” interactions dependent upon orbital overlap (section 2).

The channels II of Figure 4 are also operative in LH2.⁴⁷ The coupling in this case has the form given in eq 24, where the dominant terms at most separations are independent of orbital overlap. The Coulombic contribution to the coupling has been examined previously and shown to be complex.²⁹ The polarizability-dependent term is expected to be reasonably significant, considering the observations of polarizability and polarity sensitivity of carotenoids.^{67–69} We are currently investigating this coupling in more detail.

It is of interest to explore further the Car–Car and Car–Bchl couplings as given in eqs 20 and 24, respectively. They each involve a Coulombic coupling, although different terms in the multipole expansion contribute in either case, but a significant interaction which depends upon interchromophore orbital overlap contributes only to eq 24. The most significant common feature identified here for these two classes of interaction are the terms involving carotenoid polarizability: u^{disp} and u^{pol} . Each of these terms is related closely to the dispersion (van der Waals) interaction between ground state chromophores, but with significant enhancement owing to an electronic resonance. Approximate expressions for the overlap-independent contributions of each equation are given in eqs 25 and 26 respectively:

$$u^{\text{Coul}} \approx \frac{1}{4\pi\epsilon_0} \left[\frac{m_c m_d}{c^2 R^3} - \frac{\Theta_c \Theta_d}{R^5} \right] \quad (25a)$$

$$u^{\text{disp}} \approx \frac{-|\mu_c|^2 |\mu_d|^2}{(4\pi\epsilon_0)^2 A R^6} \quad (25b)$$

$$u^{\text{Coul}} \approx \frac{1}{4\pi\epsilon_0} \left[\frac{m_c \mu_b}{c \lambda R^2} - \frac{\Theta_c \mu_a}{R^4} \right] \quad (26a)$$

$$u^{\text{pol}} \approx \frac{-\mu_c^2 \mu_b e}{(4\pi\epsilon_0)^2 A R^5} \quad (26b)$$

where all quantities are in S.I. units and a severe, point–dipole approximation has been imposed. Electric dipole (μ), electric quadrupole (Θ), and magnetic dipole (m) transition moments are labeled with a subscript c or d to denote carotenoids, or b to denote Bchl, R is the center-to-center separation of donor and acceptor, A is the energy gap A_{57} of eq 22, and e is the elementary charge. Note that the multipole transition moments are taken only up to electric quadrupole for Car and electric dipole for Bchl. Orientation factors are set to unity (the magnetic dipole–electric quadrupole contribution to eq 25a is

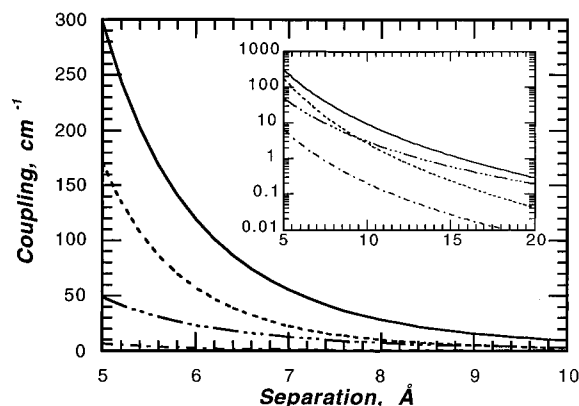


Figure 9. Evaluation of the terms contributing to eqs 20 and 24 for Car–Car and Car–Bchl coupling, respectively. The magnitude of each term is estimated using the expressions in eqs 25 and 26 with parameters typical of LH2. From the top of the main plot: the solid line represents u^{pol} , the dashed line u^{disp} , dash-dots u^{Coul} (Car–Bchl) and dash-dot u^{Coul} (Car–Car).

zero by symmetry) and the overlap-dependent contribution to eq 24 is ignored (since we will consider quite large values of R only).

In order to examine the relative significance of each term in eqs 20 and 24, and therefore Car–Car and Car–Bchl coupling, respectively, we use data typical of photosynthetic carotenoids and Bchl *a*. This is very approximate, and sufficient account has not been taken for specific properties of the chromophores involved so that, for example, individual carotenoids cannot be specified. (However, the theory may be better applied using a distributed multipole analysis, rather than the point–dipole approximation.) Thus we put $A \approx E(S_2) - E(T_1)$ [or $\approx 2E(S_1) - E(S_2)$] $\approx 14\,000\text{ cm}^{-1}$ (e.g. ref 39), λ (the reduced wavelength) $\approx 1/(17\,000\text{ cm}^{-1})$ and make use of the approximate relationship $m/c \approx \mu/137$. The carotenoid quadrupole transition moment is taken to be that calculated by Nagae et al.:²⁹ $\Theta_c \approx 6.7 \times 10^{-40}\text{ C m}^2$. The Car and Bchl dipole transition moments estimated in ref 29 appear, in relation to some of our previous studies,^{9,11,15} to be quite large, so in order to present a more conservative estimate of u^{disp} and u^{pol} , we use here approximately half those values: $\mu_c \approx 2 \times 10^{-29}\text{ C m}$ and $\mu_b \approx 1 \times 10^{-29}\text{ C m}$. For a more quantitative calculation the monopole approximation could be used for the transition moments and for the charge, e , in eq 26b.

The results are plotted in Figure 9, where R is the center-to-center separation between two arbitrary carotenoid molecules in a sandwich arrangement. Note that Figure 9 (and Figure 7) put all interactions on equal footing so as to compare *relative* magnitudes. However, the actual magnitude of these interactions will vary greatly depending upon specific properties of the system. The interactions involving the carotenoid magnetic dipole transition moment were found to be negligible in comparison to those involving the electric quadrupole transition moment (cf. ref 52). We find that each Car–Bchl coupling term is larger than its Car–Car coupling counterpart and the dominant interaction at intermediate separations in each case is u^{pol} and u^{disp} , respectively. The u^{pol} is found to have a substantial magnitude. Some of this is due to the approximations inherent in eq 26b, but the suggestion is that Car to Bchl energy transfer can be fast even at quite large separations.

Studies of the B800 to B850 energy transfer demonstrate that the rate is dependent upon a spectral overlap integral,^{70,71} as expected from eq 1, and that the transfer time is 1.2 ps at 77 K.⁷² Differentiation between the various electronic mechanisms is not possible from these experimental data; however, given that the B800–B850 separation is approximately 18 Å, a dipole–dipole coupling would seem to be a reasonable ap-

proximation for channel III of Figure 4. Jimenez et al.¹⁸ have examined this in detail.

A further possibility suggested in Figure 4 is that a superexchange^{9,73–75} pathway involving the carotenoid(s) could be significant. The initial and final singlet excited states (i.e., of the Bchl *a* chromophores) involve singly-excited configurations, thus the overall coupling would be of the “normal” type, and could involve significant contributions from the through-configuration interaction (i.e., orbital overlap dependent interactions involving the charge transfer configurations). Given the polarizability of the carotenoid and the close proximity of the carotenoid to Bchl *a* chromophores in the B800 and B850 complexes (Figure 8), this could be an important mechanism which we are currently attempting to characterize.

7. Conclusions

The origin and distance dependence of the electronic interactions which promote energy transfer within photosynthetic light-harvesting complexes has been investigated. A model based on localized molecular orbitals (summarized in section 2) was related to canonical molecular orbital calculations in section 3. This is a key step toward developing a general methodology for using CAS-SCF canonical MO calculations to determine properly the coupling between donor–acceptor pairs. This framework was used also to interpret the CAS-SCF dimer wave functions from the coupling calculations reported section 5. Sections 4 and 5 focus on the mechanism of energy transfer involving the carotenoid 2^1A_g (S_1) electronic state: [carotenoid (2^1A_g) (Car) to carotenoid (2^1A_g)] and [carotenoid (2^1A_g) to bacteriochlorophyll (Q_y) (Bchl)] interactions. The Car–Car coupling was found to involve reasonably long-range interaction terms, with a primary contribution from dispersion-type interactions, which have an R^{-6} distance dependence. The primary contributor to the Car–Bchl $S_1 \rightarrow S_1$ energy transfer mechanism was suggested to be proportional to the product of dipole–dipole and polarization interactions. In neither case does the electronic interaction resemble the Dexter exchange integral in origin or distance dependence. Some model CAS-SCF calculations of electronic interactions in 2,4,6-octatriene dimers were reported in section 5, which support the predictions of the theory for Car–Car-type coupling: The calculated interactions was found to be (i) small in comparison to the overlap-dependent triplet–triplet interaction at close separations; (ii) small in comparison to a dipole–dipole interaction (i.e., $2J$, where $J = \langle a'a|bb' \rangle$ is the Coulombic integral) at all separations; and (iii) quite weakly distance-dependent at larger separations. Figure 9 suggests that the novel dispersion and polarization-type interactions (u^{disp} and u^{pol}) of eqs 20 and 24 provide the most significant contribution to the coupling in Car–Car and Car–Bchl energy transfer, respectively. Finally, the results were related to interactions involved in LH2 through a discussion of Figure 4, given in section 6.

Acknowledgment. G.D.S. gratefully acknowledges the support of the Ramsay Memorial Fellowship Trust. Dr. Steve Bradforth and Dr. Ian Gould are thanked for valuable discussions.

References and Notes

- (1) Förster, Th. In *Modern Quantum Chemistry*; Sinanoglu, O., Ed.; Academic Press: New York, 1965; Vol. 3.
- (2) Dexter, D. L. *J. Chem. Phys.* **1953**, *21*, 836. (b) Merrifield, R. E. *J. Chem. Phys.* **1955**, *23*, 402. (c) Naqvi, K. R.; Steel, C. *Chem. Phys. Lett.* **1970**, *6*, 29. (d) Harcourt, R. D.; Ghiggino, K. P.; Scholes, G. D.; Speiser, S. *J. Chem. Phys.* **1996**, *105*, 1897.
- (3) Andrews, D. L. *Chem. Phys.* **1989**, *135*, 195.
- (4) Toledano, E.; Rubin, M. B.; Speiser, S. *J. Photochem. Photobiol., A. Chem.* **1996**, *94*, 93. (b) van Dantzig, N. A.; Levy, D. H.; Vigo, C.;

- Piotrowiak, P. *J. Chem. Phys.* **1995**, *103*, 4894. (c) Wang, Y. S.; Schanze, K. S. *Inorg. Chem.* **1994**, *33*, 1354.
- (5) Fleming, G. R.; van Grondelle, R. *Phys. Today* **1994**, 48.
- (6) Osuka, A.; Nakajima, S.; Okada, T.; Taniguchi, S.; Nozaki, K.; Ohno, T.; Yamazaki, I.; Nishimura, Y.; Mataga, N. *Angew. Chem., Int. Ed. Engl.* **1996**, *35*, 92.
- (7) Hess, S.; Åkesson, E.; Cogdell, R. J.; Pullerits, T.; Sundström, V. *Biophys. J.* **1995**, *69*, 2211.
- (8) Du, M.; Xie, M.; Mets, L.; Fleming, G. R. *J. Phys. Chem.* **1994**, *98*, 4736. (b) Bradforth, S. E.; Jimenez, R.; van Mourik, F.; van Grondelle, R.; Fleming, G. R. *J. Phys. Chem.* **1995**, *99*, 16179.
- (9) Scholes, G. D.; Ghiggino, K. P.; Oliver, A. M.; Paddon-Row, M. N. *J. Phys. Chem.* **1993**, *97*, 11871.
- (10) Scholes, G. D.; Ghiggino, K. P.; Oliver, A. M.; Paddon-Row, M. N. *J. Am. Chem. Soc.* **1993**, *115*, 4345.
- (11) Scholes, G. D.; Ghiggino, K. P. *J. Phys. Chem.* **1994**, *98*, 4580. Note the following corrections in eqs 7: eq 7e replace $(ab|ab')$ with $(ab|a'b')$, Eq. (7f) replace $2(a'|a)$ with $(a'|a')t$, and eq 7g replace $3(aa|bb)q + (aa|a'b')$ with $2(aa|bb)q + 3(aa|a'b')$.
- (12) Harcourt, R. D.; Scholes, G. D.; Ghiggino, K. P. *J. Chem. Phys.* **1994**, *101*, 10521.
- (13) Scholes, G. D.; Harcourt, R. D.; Ghiggino, K. P. *J. Chem. Phys.* **1995**, *102*, 9754.
- (14) Scholes, G. D.; Harcourt, R. D. *J. Chem. Phys.* **1996**, *104*, 5054.
- (15) Scholes, G. D. *J. Phys. Chem.* **1996**, *100*, 18731.
- (16) McDermott, G.; Prince, S. M.; Freer, A. A.; Hawthornethwaite-Lawless, A. M.; Papiz, M. Z.; Cogdell, R. J.; Isaacs, N. W. *Nature* **1995**, *374*, 517. (b) Freer, A. A.; Prince, S. M.; Sauer, K.; Papiz, M. Z.; Hawthornethwaite-Lawless, A. M.; McDermott, G.; Cogdell, R. J.; Isaacs, N. W. *Structure* **1996**, *4*, 449.
- (17) Karrasch, S.; Bullough, P. A.; Ghosh, R. *EMBO J.* **1995**, *14*, 631.
- (18) Jimenez, R.; Dikshit, S. N.; Bradforth, S. E.; Fleming, G. R. *J. Phys. Chem.* **1996**, *100*, 6825.
- (19) De Caro, C.; Visschers, R. W.; van Grondelle, R.; Völker, S. J. *J. Phys. Chem.* **1994**, *98*, 10584.
- (20) Valkunas, L.; Åkesson, E.; Pullerits, T.; Sundström, V. *Biophys. J.* **1996**, *70*, 2373. (b) Pullerits, T.; Visscher, K. J.; Hess, S.; Sundström, V.; Freiberg, A.; Timpmann, K.; van Grondelle, R. *Biophys. J.* **1994**, *66*, 236.
- (21) Pullerits, T.; Sundström, V. *Acc. Chem. Res.* **1996**, *29*, 281.
- (22) Pullerits, T.; Chachisvilis, M.; Sundström, V. *J. Phys. Chem.* **1996**, *100*, 10787. (b) Kennis, J. T. M.; Steltsov, A. M.; Aartsma, T. J.; Nozawa, T.; Amez, J. *J. Phys. Chem.* **1996**, *100*, 2438.
- (23) Savikhin, S.; Struve, W. S. *Biochemistry* **1994**, *33*, 11200.
- (24) Durrant, J. R.; Klug, D. R.; Kwa, S. L. S.; van Grondelle, R.; Porter, G.; Dekker, J. P. *Proc. Natl. Acad. Sci. U.S.A.* **1995**, *92*, 4798.
- (25) Frank, H. A.; Cogdell, R. J. In *Carotenoids in Photosynthesis*; Young, A.; Britton, G., Eds.; Chapman and Hall: London, 1993; p 252.
- (26) Koyama, Y. *J. Photochem. Photobiol. B Biol.* **1991**, *9*, 265.
- (27) Shreve, A. P.; Trautman, J. K.; Frank, H. A.; Owens, T. G.; Albrecht, A. C. *Biochim. Biophys. Acta* **1991**, *1058*, 280.
- (28) Ricci, M.; Bradforth, S. E.; Jimenez, R.; Fleming, G. R. *Chem. Phys. Lett.* **1996**, *259*, 281.
- (29) Nagae, H.; Kakitani, T.; Katoh, T.; Mimuro, M. *J. Chem. Phys.* **1993**, *98*, 8012.
- (30) Scholes, G. D.; Ghiggino, K. P. *J. Chem. Phys.* **1994**, *101*, 1251.
- (31) Lin, S. H. *Mol. Phys.* **1971**, *21*, 853. (b) Lin, S. H.; Xiao, W. Z. *Phys. Rev. E* **1993**, *47*, 3698.
- (32) Mukamel, S. *Principles of Nonlinear Optical Spectroscopy*; Oxford University Press: New York, 1995.
- (33) Mukamel, S.; Rupasov, V. *Chem. Phys. Lett.* **1995**, *242*, 17.
- (34) Scholes, G. D.; Clayton, A. H. A. C.; Ghiggino, K. P. *J. Chem. Phys.* **1992**, *97*, 7405.
- (35) Closs, G. L.; Piotrowiak, P.; MacInnis, J. M.; Fleming, G. R. *J. Am. Chem. Soc.* **1988**, *110*, 2652. (b) Closs, G. L.; Johnson, M. D.; Miller, J. R.; Piotrowiak, P. *J. Am. Chem. Soc.* **1989**, *111*, 3751.
- (36) Clayton, A. H.; Scholes, G. D.; Ghiggino, K. P.; Paddon-Row, M. N. *J. Phys. Chem.* **1996**, *100*, 10912.
- (37) Koutecký, J.; Paldus, J. *Theor. Chim. Acta (Berlin)* **1963**, *1*, 268. (b) Koutecký, J.; Paldus, J. *Collect. Czech. Chem. Commun.* **1962**, *27*, 599.
- (c) Polák, R.; Paldus, J. *Theor. Chim. Acta (Berlin)* **1966**, *4*, 37.
- (38) Fidler, H.; Terpstra, J.; Wiersma, D. A. *J. Chem. Phys.* **1991**, *94*, 6895.
- (39) Koyama, Y.; Kuki, M.; Andersson, P. O.; Gillbro, T. *Photochem. Photobiol.* **1996**, *63*, 243.
- (40) Frank, H. A.; Cogdell, R. J. *Photochem. Photobiol.* **1996**, *63*, 257.
- (41) Gillbro, T.; Andersson, P. O.; Liu, R. S. H.; Asato, A. E.; Takaishi, S.; Cogdell, R. J. *Photochem. Photobiol.* **1993**, *57*, 44.
- (42) Frank, H. A.; Farhoosh, R.; Aldema, M. L.; DeCoster, B.; Christensen, R. L.; Gebhard, R.; Lugtenburg, J. *Photochem. Photobiol.* **1993**, *57*, 49.
- (43) Cogdell, R. J.; Frank, H. A. *Biochim. Biophys. Acta* **1987**, *895*, 63.
- (44) Mimuro, M.; Katoh, T. *Pure Appl. Chem.* **1991**, *63*, 123.
- (45) Tavan, P.; Schulten, K. *Phys. Rev. B* **1986**, *36*, 4337. (b) Tavan, P.; Schulten, K. *J. Chem. Phys.* **1986**, *85*, 6602.
- (46) DeCoster, B.; Christensen, R. L.; Gebhard, R.; Lugtenburg, J.; Farhoosh, R.; Frank, H. A. *Biochim. Biophys. Acta* **1992**, *1102*, 107.
- (47) Andersson, P. O.; Cogdell, R. J.; Gillbro, T. *Chem. Phys.* **1996**, *210*, 195.
- (48) Hayashi, H.; Kolaczowski, S. V.; Nuguchi, T.; Blanchard, D.; Atkinson, G. H. *J. Am. Chem. Soc.* **1990**, *112*, 4664.
- (49) Prince, S. M.; McDermott, G.; Freer, A. A.; Hawthornthwaite-Lawless, A. M.; Papiz, M. Z.; Isaacs, N. W.; Cogdell, R. J. In *Abstracts of the 6th Congress of the European Society for Photobiology*; Cambridge University Press: London, 1995; p 2.
- (50) Scholes, G. D.; Andrews, D. L. *J. Chem. Phys.*, in press.
- (51) London F. Z. *Phys.* **1930**, *63*, 245.
- (52) Craig, D. P.; Thirunamachandran, T. *Molecular Quantum Electrodynamics*; Academic Press: New York, 1984.
- (53) Andrews, D. L. *Faraday Discuss.* **1994**, *99*, 375.
- (54) Power, E. A.; Thirunamachandran, T. *Phys. Rev. A* **1993**, *48*, 4761.
- (b) Power, E. A.; Thirunamachandran, T. *Phys. Rev. A* **1995**, *51*, 3660. (c) Power, E. A.; Thirunamachandran, T. *Chem. Phys.* **1995**, *198*, 5.
- (55) McWeeny, R. *Methods of Molecular Quantum Mechanics*, 2nd ed.; Academic Press: New York, 1992.
- (56) Bernardi, F.; Bottini, A.; McDougall, J. J. W.; Robb, M. A.; Schlegel, *Faraday Symp. Chem. Soc.* **1984**, *19*, 137.
- (57) Roos, B. O.; Andersson, K.; Fülcher, M. P. *Chem. Phys. Lett.* **1992**, *192*, 5.
- (58) *Gaussian 94*, Revision C.2; Frisch, M. J.; Trucks, G. W.; Schlegel, H. B.; Gill, P. M. W.; Johnson, B. G.; Robb, M. A.; Cheeseman, J. R.; Keith, T.; Petersson, G. A.; Montgomery, J. A.; Raghavachari, K.; Al-Laham, M. A.; Zakrzewski, V. G.; Ortiz, J. V.; Foresman, J. B.; Cioslowski, J.; Stefanov, B. B.; Nanayakkara, A.; Challacombe, M.; Peng, C. Y.; Ayala, P. Y.; Chen, W.; Wong, M. W.; Andres, J. L.; Replogle, E. S.; Gomperts, R.; Martin, R. L.; Fox, D. J.; Binkley, J. S.; Defrees, D. J.; Baker, J.; Stewart, J. P.; Head-Gordon, M.; Gonzalez, C.; Pople, J. A. *Gaussian, Inc.*: Pittsburgh, PA, 1995.
- (59) Serrano-Andrés, L.; Lindh, R.; Roos, B. O. *J. Phys. Chem.* **1993**, *97*, 9360.
- (60) Buma, W. J.; Kohler, B. E.; Song, K. *J. Chem. Phys.* **1991**, *94*, 4691.
- (61) Kramer, H. J. M.; van Grondelle, R.; Hunter, N.; Westerhuis, W. H. J.; Amez, J. *Biochim. Biophys. Acta* **1984**, *765*, 156.
- (62) Chadwick, B. W.; Zhang, C.; Cogdell, R. J.; Frank, H. A. *Biochim. Biophys. Acta* **1987**, *893*, 444.
- (63) Frank, H. A.; Cua, A.; Chynwat, V.; Young, A.; Gortzola, D.; Wasielewski, M. *Photosynth. Res.* **1994**, *41*, 389.
- (64) Trautman, J. K.; Shreve, A. P.; Violette, C. A. *Proc. Natl. Acad. Sci. U.S.A.* **1990**, *87*, 215.
- (65) Shreve, A. P.; Trautman, J. K.; Frank, H. A.; Owens, T. G.; Albrecht, A. C. *Biochim. Biophys. Acta* **1991**, *1058*, 280.
- (66) Krueger, B.; Scholes, G. D.; Jimenez, R.; Fleming, G. R., manuscript in preparation.
- (67) Crielaard, W.; Visschers, R. W.; Fowler, G. J. S.; van Grondelle, R.; Hellingwerf, K. J.; Hunter, C. N. *Biochim. Biophys. Acta* **1994**, *1183*, 473.
- (68) Gottfried, D. S.; Steffen, M. A.; Boxer, S. G. *Science* **1991**, *251*, 662.
- (69) Gottfried, D. S.; Steffen, M. A.; Boxer, S. G. *Biochim. Biophys. Acta* **1991**, *1059*, 76.
- (70) Hess, S.; Visscher, K. J.; Pullerits, T.; Sundström, V.; Fowler, G. J. S.; Hunter, C. N. *Biochemistry* **1994**, *33*, 8300.
- (71) Wu, H.-M.; Savikhin, S.; Reddy, N. R. S.; Jankowiak, R.; Cogdell, R. J.; Struve, W. S.; Small, G. J. *J. Phys. Chem.* **1996**, *100*, 12022.
- (72) Monshouwer, R.; de Zarate, O. I.; van Mourik, F.; van Grondelle, R. *Chem. Phys. Lett.* **1995**, *246*, 341.
- (73) Newton, M. D. *Chem. Rev.* **1991**, *91*, 767.
- (74) Jordan, K. D.; Paddon-Row, M. N. *Chem. Rev.* **1992**, *92*, 395.
- (75) Hu, Y.; Mukamel, S. *J. Chem. Phys.* **1989**, *91*, 6973.